ORIGINAL PAPER

Gallium Oxide Growth

physica status solidi a

www.pss-a.com

Towards High-Mobility Heteroepitaxial β-Ga_2O_3 on Sapphire — Dependence on The Substrate Off-Axis Angle

*Subrina Rafique, Lu Han, Adam T. Neal, Shin Mou, John Boeckl, and Hongping Zhao**

This paper presents the heteroepitaxial growth of β-Ga_2O_3 thin films on off-axis (0001) c-sapphire substrates by low pressure chemical vapor deposition (LPCVD). (−201) oriented β-Ga_2O_3 thin films are grown using high purity metallic gallium (Ga) and oxygen (O_2) as the precursors. N-type conductivity in silicon doped β-Ga_2O_3 thin films is demonstrated. It is found that the film crystalline quality, surface morphology, and electrical conductivity are remarkably sensitive to the off-axis angles. X-ray phi-scan measurements of the β-Ga_2O_3 film grown on on-axis c-sapphire indicate the presence of six in-plane rotational domains due to the substrate symmetry. With the increase of off-axis angle toward <11–20> of sapphire, one of the in-plane orientations is strongly favored. The use of off-axis substrate also reduced the X-ray rocking curve full width at half maximum and increased the intensities of the Raman peaks. The best electrical properties of the β-Ga_2O_3 film are exhibited by the film grown on 6° off-axis c-sapphire. The room temperature electron Hall mobility was 106.6 $cm^2 V^{-1} s^{-1}$ with an n-type carrier concentration of 4.83×10^{17} cm^{-3}. The results from this study demonstrate high electrical quality β-Ga_2O_3 thin films grown on off-axis c-sapphire substrates, which are promising for high power electronic and short wavelength optoelectronic device applications.

1. Introduction

Gallium oxide (Ga_2O_3) was used as a transparent conducting oxide (TCO),[1] and only very recently was studied as an emerging ultrawide band gap (UWBG) semiconductor with a room temperature energy gap of ≈4.5–4.9 eV, larger than those of the counterparts SiC (≈3.2 eV) and GaN (≈3.4 eV). It possesses excellent chemical and thermal stability up to 1400 °C. Due to the very large band gap, it has an estimated breakdown field of ≈6–8 MV cm^{-1} and high transparency in the deep ultraviolet (UV) and visible wavelength region. Another advantage lies in the feasibility to mass produce high quality bulk Ga_2O_3 at low cost using melting growth techniques such as edge defined film-fed growth (EFG),[2] floating zone (FZ),[3] and Czochralski[4] methods. Ga_2O_3 can also be used as a conductive and transparent substrate for GaN based light emitting diodes (LEDs). The intrinsic unique properties of Ga_2O_3 make it a promising candidate for high power electronic and short wavelength optoelectronic device applications.

Several epitaxial growth techniques for β-Ga_2O_3 thin films such as molecular beam epitaxy (MBE),[5] metal organic vapor phase epitaxy (MOVPE),[6] halide vapor phase epitaxy (HVPE),[7] and low pressure chemical vapor deposition (LPCVD)[8] have been reported recently. The current efforts focus on β-Ga_2O_3 homoepitaxial growth on native substrates as it is expected to produce high quality materials for device applications.[9–12] At present, 2-inch diameter β-Ga_2O_3 wafers are commercially offered from Tamura, Inc. (Japan), but they are only available in the (−201) crystal orientation. Wafers with 10×15 mm^2 dimensions having (010) and (001) crystal orientations are also available commercially. The wafer sizes of these orientations are currently limited by the pulling direction of EFG grown β-Ga_2O_3 bulk single crystal. In addition, the as-grown unintentional doped (UID) Ga_2O_3 substrates are conductive due to the existence of the Si impurity which serves as n-type dopant. Magnesium (Mg) and iron (Fe) have been used as dopants to convert the conductive Ga_2O_3 to semi-insulating substrates. Nevertheless, studies of heteroepitaxy of β-Ga_2O_3 thin films on

S. Rafique, Dr. L. Han, Prof. H. Zhao
Department of Electrical Engineering and Computer Science
Case Western Reserve University,
Cleveland, OH 44106, USA
E-mail: zhao.2592@osu.edu

Dr. A. T. Neal, Dr. S. Mou, Dr. J. Boeckl
Air Force Research Laboratory, Materials and Manufacturing Directorate, Wright-Patterson Air Force Base,
OH 45433, USA

Dr. A. T. Neal
Universal Technology Corporation,
Dayton, OH 45432, USA

Prof. H. Zhao
Department of Electrical and Computer Engineering
The Ohio State University,
Columbus, OH 43210, USA

Prof. H. Zhao
Department of Materials Science and Engineering
The Ohio State University,
Columbus, OH 43210, USA

DOI: 10.1002/pssa.201700467

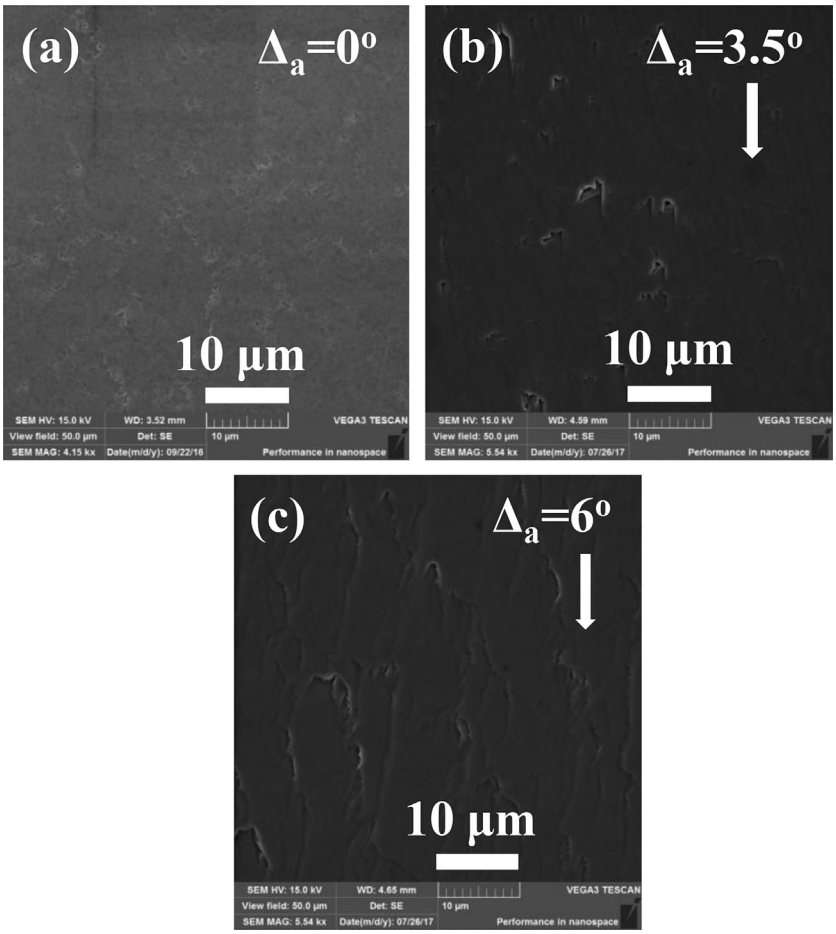

Figure 1. Top view SEM images of β-Ga_2O_3 thin films grown on c-plane (0001) sapphire substrates with different off-angles toward <11–20>. a) $\Delta_a = 0°$. b) $\Delta_a = 3.5°$. c) $\Delta_a = 6°$. The off-cut directions are indicated by the white arrows. The thin films have a thickness of ≈6 µm.

low cost and large area foreign substrates such as sapphire are important both scientifically and technologically.

Heteroepitaxial growth of β-Ga_2O_3 thin films on Al_2O_3,[13–16] Si,[17] MgO,[18,19] and ZrO_2:Y[20] have been reported previously in the literature. However, it is still challenging to obtain high-quality Ga_2O_3 layers on foreign substrates due to their large lattice mismatches and crystal asymmetry between them. A high density of defects and dislocations form at the interface, some of which may thread into the epilayers. These thin films are usually highly textured and have in-plane rotational domains limiting their semiconductor material properties. Therefore, there is a great need for an in-depth investigation of parameters that exert impacts on the properties of the β-Ga_2O_3 thin films grown on foreign substrates such as sapphire.[21]

Small off-angled substrates are often utilized to improve the crystallinity of epitaxial thin films,[22] because they are usually believed to enhance step flow growth of thin films and control domain structures. The atomic steps on the surface of the off-angled substrates act as the preferential binding sites for the incoming adatoms promoting the step flow growth. The growth of heteroepitaxial β-Ga_2O_3 thin films by HVPE on off-angled sapphire substrates has been studied and reported previously.[21] However, electrical properties of those films were not discussed. In this paper, we present the heteroepitaxial growth of n-type Si doped β-Ga_2O_3 thin films on c-plane sapphire substrates with different off-axis angles toward <11–20> direction by LPCVD. Comprehensive studies of the effects of the sapphire substrate misorientation on the surface morphology, crystal quality and orientation, and electrical properties of the as-grown β-Ga_2O_3 thin films were conducted.

2. Experimental Section

2.1. Growth of β-Ga_2O_3 Thin Film

The growth of β-Ga_2O_3 thin films was carried out in a low pressure chamber equipped with programmable temperature controller. Off-axis c-plane sapphire substrates with off-axis angles in the range between 0° to 10° toward sapphire <11–20> (Δ_a) were used. The substrates were cleaned with solvents, rinsed by de-ionized water and dried with nitrogen flow before growth. High purity gallium pellets (Alfa Aesar, 99.99999%) and oxygen (O_2) gas were used as the precursors for gallium and oxygen, respectively. Ultra-high purity Argon (Ar) was used as the carrier gas. The growths were carried out at 900 °C at an oxygen volume percentage of 4.8%. $SiCl_4$ was used as an n-type dopant gas. The thin film doping concentration was varied by changing the dopant flow rate. For all the above mentioned

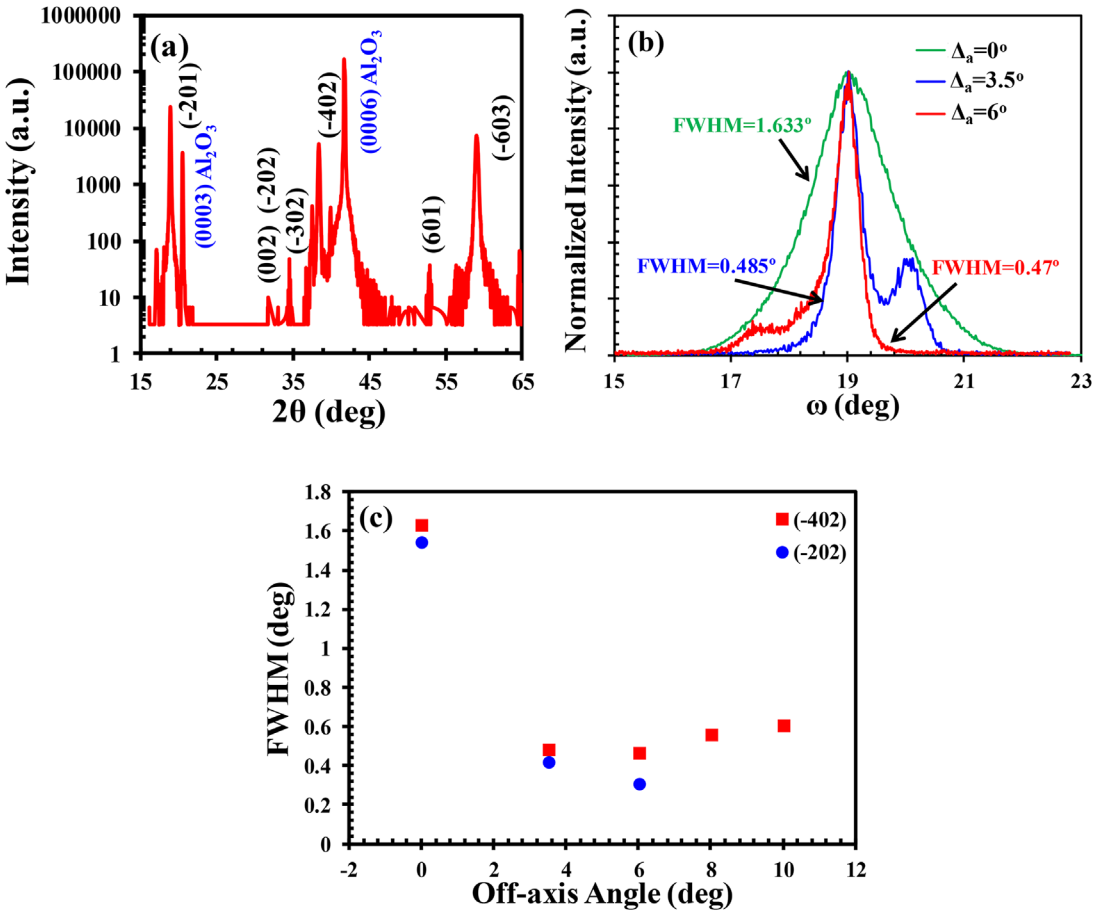

Figure 2. a) XRD pattern (2θ scan) of a β-Ga_2O_3 thin film grown on c-plane (0001) sapphire substrate with no off-angle. b) XRD rocking curves of symmetric (−402) reflection peaks of β-Ga_2O_3 thin films grown on c-plane (0001) sapphire substrates with different off-angles toward <11–20>. c) Dependence of the FWHM values of the symmetric (−402) and asymmetric (−202) diffraction peaks on the off-axis angles. The thin films have a thickness of ≈6 μm.

growths, the growth pressure was kept at 4 Torr. Controllable growth rates of β-Ga_2O_3 thin films ranging between 0.5–10 μm hr^{-1} have been achieved via our developed LPCVD growth method by tuning the growth parameters such as growth temperature, growth pressure and precursor flow rate. The growth rate and the crystallinity of the thin films did not show obvious degradation for the range of the carrier concentration studied here.

2.2. Characterization of β-Ga_2O_3 Thin Film

The structure, crystal quality and electrical properties of the β-Ga_2O_3 thin films were characterized by using scanning electron microscopy (SEM), X-ray diffraction (XRD), and van der Pauw/Hall measurement. The SEM images were taken with Tescan Vega-3. XRD spectra and phi scans were collected on a Bruker Discover D8 X-Ray Diffractometer with Cu Kα radiation (1.54 Å). The Raman spectra were taken at room temperature using a 532 nm laser at a power of 300 μW. The beam was focused using a 100x microscope objective and typical spot size was ≈1 μm. Transmission electron microscopy (TEM) samples were prepared using a focused ion beam (FIB) lift-out technique. Prior to ion milling, the samples were protected with a Pt cap of ≈2 μm to preserve the initial surface integrity. The samples were then prepared by FIB milling with a Ga ion beam to a thickness of ≈1 μm and then polished using an Ar ion beam to remove the Ga ion damage and to obtain electron transparency for high resolution imaging. TEM characterization of the film was performed using an aberration corrected (image) Titan 80–300 TEM operated at an accelerating voltage of 300 kV. The carrier concentration and electron Hall mobility were measured with HMS 3000 Hall measurement system. Temperature dependent Hall measurement was carried out using two custom built systems. An electromagnet with a vacuum cryostat with closed-cycle He refrigerator was used for below room temperature measurement. For above room temperature measurement, an electromagnet with a quartz tube and silicon carbide heater was used. Nitrogen gas was used to purge the quartz tube during high temperature measurements.

3. Results and Discussion

To illustrate the effect of off-axis c-plane sapphire substrate on the surface topography of β-Ga_2O_3 thin films, SEM was

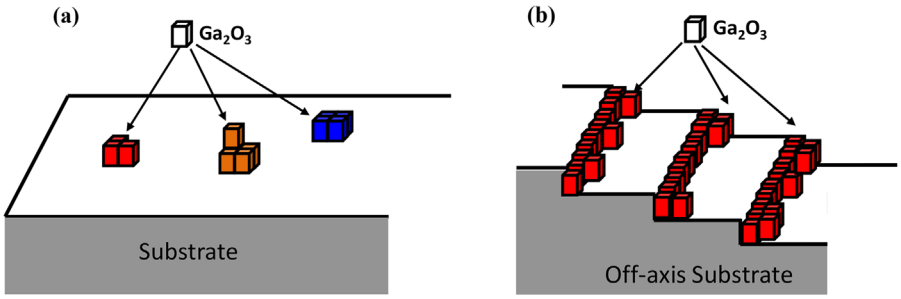

Figure 3. Schematic illustrations of the proposed growth mechanisms of β-Ga_2O_3 thin films grown on (0001) c-plane sapphire substrates: (a) without off-axis; and (b) with off-axis angles.

conducted. The images are shown in **Figure 1**. For the sapphire substrate with 0° off-axis angle, the thin film is composed of small pseudo hexagonal rotational domains. In the case of sapphire substrates with off-axis angles (3.5° and 6°), the domains are well aligned along the direction of off-cut as can be seen in Figure 1b and c which is due to the step flow growth mode promoted by substrate misorientation.

The influence of off-axis c-plane sapphire substrate on the crystal quality of the Si-doped β-Ga_2O_3 thin films was characterized by XRD and rocking curve measurement. **Figure 2**a shows the XRD θ-2θ scan spectrum of the thin film grown on c-sapphire substrate with 0° off-axis angle. Besides the diffraction peaks of the substrate, primary reflections from {−201} family of planes of β-Ga_2O_3 are present in the spectrum. Some other very low intensity (2–3 orders lower) diffraction peaks observed in Figure 2a are negligible. This indicates that the as-grown thin film is phase pure with [−201] as the preferred growth orientation. This is because the oxygen atoms of (0001) plane of sapphire substrate has a similar atomic arrangement as the (−201) equivalent plane of β-Ga_2O_3.[23] It has been reported previously for III-nitride epitaxial films that the full width at half maximum (FWHM) values of the symmetric and asymmetric diffraction peaks are associated with screw and edge dislocations respectively.[24,25] In this study, we have performed the XRD rocking curve measurements for both symmetric (−402) and asymmetric (−202) diffraction peaks. Figure 2b shows the XRD rocking curves of the symmetric (-402) diffraction peaks. The FWHM of the rocking curves are measured as 1.633° ($\Delta_a = 0°$), 0.485° ($\Delta_a = 3.5°$), and 0.47° ($\Delta_a = 6°$), respectively. Figure 2c plots the FWHM values of the symmetric and asymmetric diffraction peaks as a function of the off-axis angle. The FWHM values for both the peaks decreased significantly

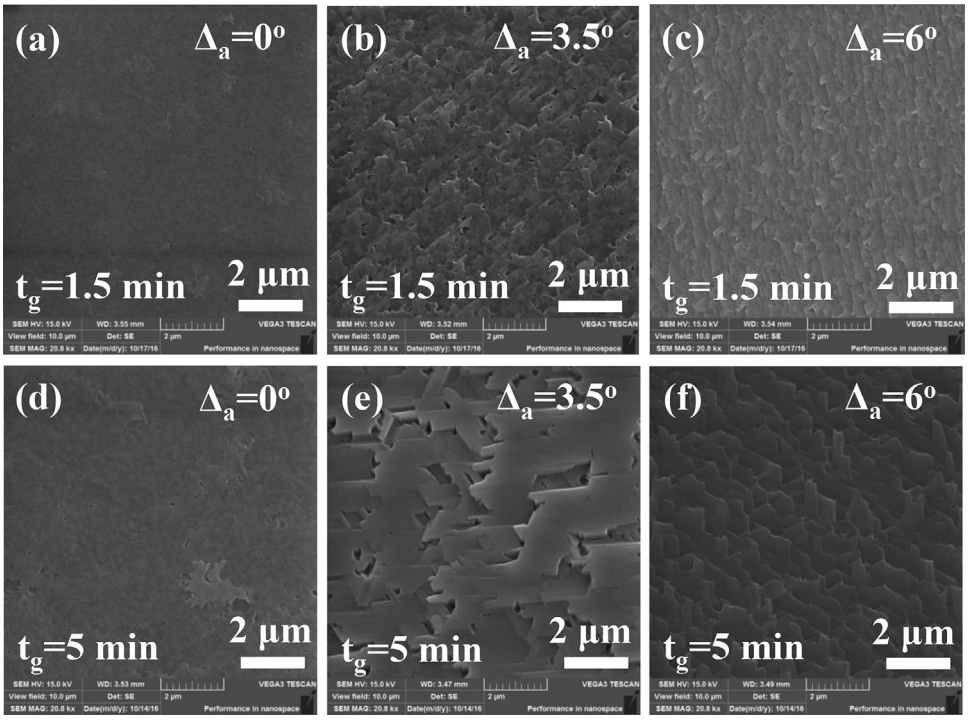

Figure 4. Top view SEM images of β-Ga_2O_3 thin films grown on c-plane (0001) sapphire substrates with different off-angles toward <11–20> for different growth times. (a–c) for 1.5 min. (d–f) for 5 min. The thicknesses of the thin films for (a–c) and (d–f) are ≈150 and ≈500 nm, respectively.

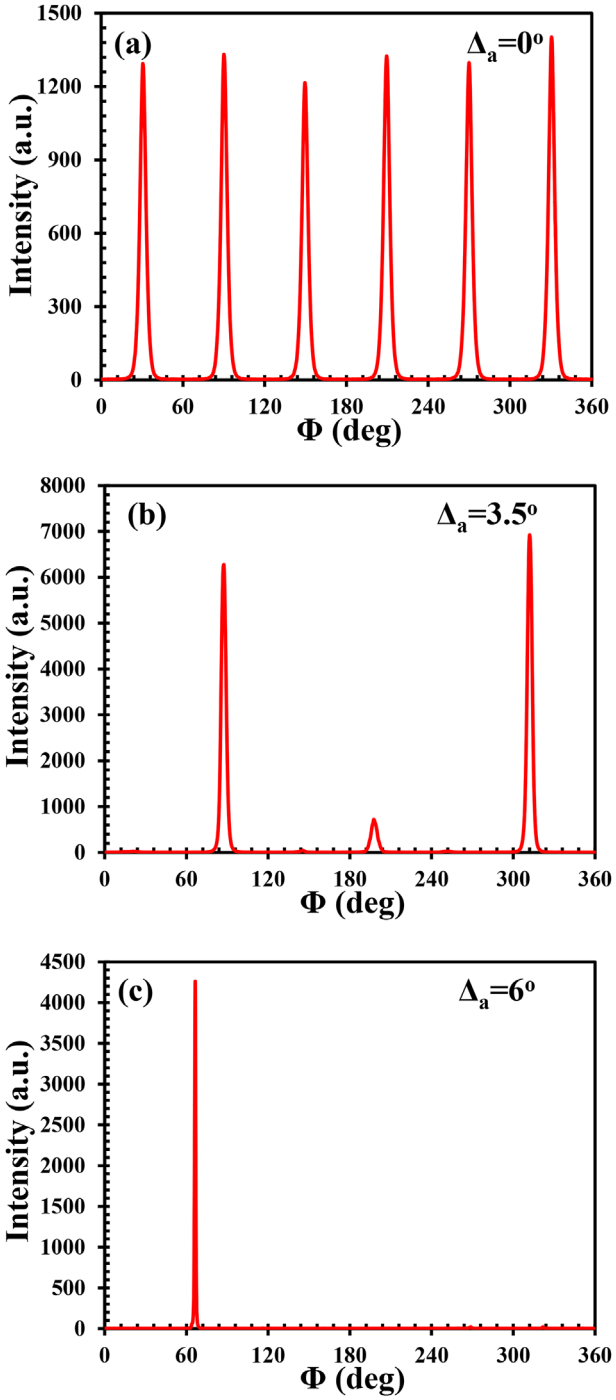

Figure 5. XRD phi scans of (−401) reflections of β-Ga_2O_3 thin films grown on c-plane (0001) sapphire substrates with different off-angles toward <11–20>. a) $\Delta_a = 0°$. b) $\Delta_a = 3.5°$. c) $\Delta_a = 6°$. The thin films have a thickness of ≈6 μm.

with increasing off-axis angle indicating larger off-cut improves the crystal quality of the β-Ga_2O_3 thin films. Note that additional crystallographic peaks other than (−402) were shown in Figure 2b, which is due to the asymmetric in-plane surfaces of the off-axis c-plane sapphire substrates. Proper optimization of the sample tilt angle during rocking curve measurement can help to get rid of such undesired peaks. However, as we further increased the off-axis angles to 8° and 10°, we observed broadening of the FWHM values to 0.56° and 0.61°, respectively. Such broadening might have occurred due to the step bunching and indicates degradation of the material quality of the thin films for off-axis angle larger than 6°. Based on these results, we concluded that for our LPCVD growth condition, 6° is the preferred off-axis angle for high quality thin film growth on c-sapphire substrate. For comparison, the reported representative FWHMs of heteroepitaxial β-Ga_2O_3 thin films grown on c-plane sapphire substrates were 0.9° (MBE, (−201) diffraction peak),[26] 0.6° (MOCVD, (−201) diffraction peak)[27] and 2.42° (MOVPE, (−402) diffraction peak).[28]

The average grain size (D) of the β-Ga_2O_3 thin films can be estimated from the FWHM of the (−402) peaks by using the Scherrer's formula[29]:

$$D = \frac{0.9\lambda}{B\cos\theta} \quad (1)$$

where λ is the X-ray wavelength, B is the FWHM of the XRD peak and θ is the diffraction angle. With increasing the off-axis angle, the estimated grain size of the β-Ga_2O_3 thin films increased from 5.1 nm ($\Delta_a = 0°$) to 17.9 nm ($\Delta_a = 6°$).

The schematic of gallium (Ga) localization mechanism during the growth of β-Ga_2O_3 thin films is shown in **Figure 3**. The thin film growth followed step flow growth mechanism on off-axis substrates. Thin film growth on vicinal substrates for other material systems have been reported previously.[30,31] Surface diffusion of adatoms and step incorporation kinetics were considered to be two key factors. For thin film growth on substrate with 0° off-axis angle, there are no preferential sites on the substrate surface for Ga adatoms to incorporate into. On the other hand, when off-axis substrate is used, steps act as the preferred incorporation sites for the Ga adatoms. This suppresses the random nucleation on the surface and step flow growth occurs along the off-cut direction. Note that the surface diffusion length of Ga which depends on the growth condition; needs to be comparable to the step terrace-width in order to sustain stable step morphology. If the step terrace-width is longer than Ga adatom surface diffusion length, island nucleation occurs on the terrace since the Ga adatoms cannot reach the step edge. The surface mobility of the adatoms might also be affected by the accommodation of the lattice mismatch between Ga_2O_3 and sapphire with the use of off-axis substrates. It has been reported previously for homoepitaxial growth of Ga_2O_3 thin films on (100) native substrates with different miscut-angles that the prevalence of the step flow growth depends on the miscut-angle for given growth conditions (temperature, flux of adatoms).[6] The step terrace-width is inversely proportional to the tangent of off-axis angle. With the increase of off-axis angle, step terrace-width decreases. As a result, Ga adatoms can easily reach the step edge and step flow growth occurs. To verify the growth mechanism of β-Ga_2O_3 thin films, growth was conducted for various dwell times. **Figure 4** shows the top view SEM images of the β-Ga_2O_3 thin films grown for 1.5 and 5 min. The results corroborate the step flow growth of the β-Ga_2O_3 thin films on the off-axis sapphire substrates.

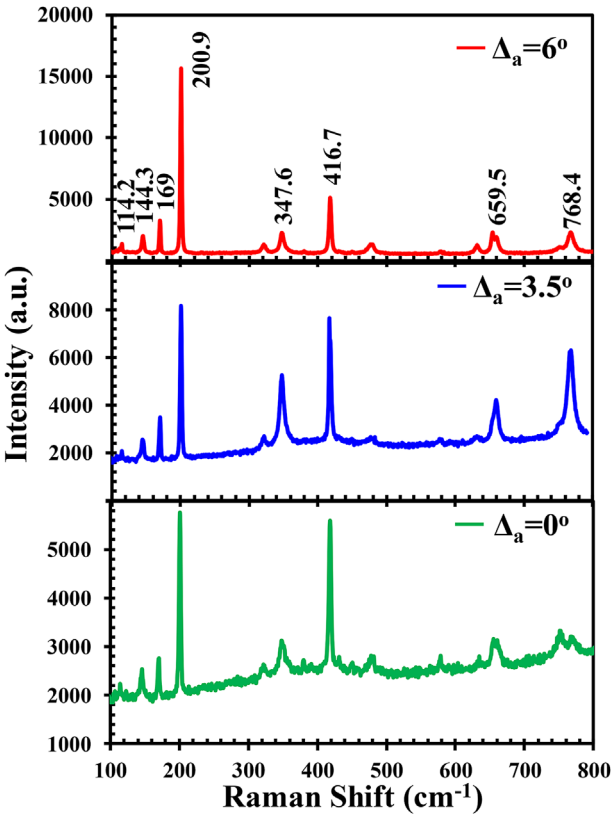

Figure 6. Micro Raman spectra of β-Ga_2O_3 thin films grown on c-plane (0001) sapphire substrates with different off-angles toward <11–20>. The thin films have a thickness of ≈6 μm.

To characterize the in-plane domain properties, the XRD phi (φ) scan spectra were taken. From **Figure 5**a, for the thin film grown on 0° off-axis substrate, six strong diffraction peaks with similar intensity were measured. The peaks are separated by 60°. The origin of these six peaks is due to the diploid symmetry of monoclinic β-Ga_2O_3 and three kinds of equivalent in-plane orientations of Ga_2O_3 grains on the substrate.[27] With the introduction of off-axis substrates, the domain structure changed dramatically. A 3.5° off-axis substrate promotes three orientations and suppresses the other three orientations as can be seen from Figure 5b. Increasing off-cut angle from 3.5° to 6° further strengthens the preferential orientation. For the thin film grown on 6° off-axis substrate, only one peak appears in the phi scan (Figure 5c). Such change in domain structure occurs because off-cut substrates introduce steps along a specified direction and breaks the equivalency on the substrate surface.

Raman spectroscopy was carried out to investigate the effect of substrate misorientation angle on the crystal quality of the β-Ga_2O_3 thin films. **Figure 6** shows the Raman spectra of the β-Ga_2O_3 thin films. Eight Raman peaks were observed for each sample. The peaks appearing at 114.2, 144.3, 169, 200.9, 347.6, 416.7, 659.5, and 768.4 cm^{-1} were blue-shifted by 0.3–2.5 cm^{-1} as compared to the bulk Raman peaks.[30] This indicates that all the films were under slight compressive strain which can be due to the lattice mismatch between Ga_2O_3 and sapphire. The strongest low frequency peak located at 200.9 cm^{-1} is the characteristic translation and libration mode of Ga-O chains [32]. The intensity of this peak is the strongest and its FWHM is the narrowest for the thin film grown on 6° off-axis compared with the ones on 3.5° and 0° off-axis substrates. This indirectly demonstrates that the thin film grown on 6° off-axis sapphire has the best crystalline quality.

Cross sectional TEM characterization were performed to investigate the effect of substrate misorientation angle on the defects of the β-Ga_2O_3 thin films. **Figure 7** shows the cross sectional TEM images of the β-Ga_2O_3 thin films. The thin film grown on 0° off-axis substrate has a high density of defects, which propagate all the way from the interface to the top of the film along the growth direction. These defects could be planar defects such as grain boundaries. However, to identify the defects accurately, further TEM studies are required. With the increase of the off-axis angle, the defects became fewer and tilted with respect to the interface. This could be due to the reduction of in plane rotational domains seen from the XRD phi scan of Figure 5. With the increase of the off-axis angle, the growth directions of the thin films were no longer perpendicular to the substrate surface and the defects became tilted with respect to the interface. For the thin film grown on 6° off-axis substrate, the defects propagate for ≈2.7 μm inside the film from the interface and then stopped. The rest of the film does not show obvious defects. Such phenomena have been previously observed for GaN thin films grown on vicinal sapphire substrates by MBE.[25] Based on the above-mentioned results, the usage of well-controlled off-axis substrates can be an effective method for reducing defect density in heteroepitaxial β-Ga_2O_3 thin films.

Room temperature Hall measurements were carried out on the as-grown β-Ga_2O_3 thin films. Van der Pauw configuration with indium-tin eutectic electrodes was used for the measurement. Indium and indium-gallium eutectic have been used previously as ohmic electrodes for Hall measurements of Ga_2O_3.[33,34] The applied magnetic field was 0.975 T. **Figure 8** plots the Hall mobility as a function of the n-type carrier concentration for the Si-doped β-Ga_2O_3 thin films. By keeping the growth condition (temperature, pressure, Ar and O_2 flow rate) fixed and varying the doping source flow rate from 0.005–0.4 sccm, the carrier concentration can be broadly tuned between low-10^{17} to low-10^{20} cm^{-3} range. The background doping concentration for an unintentionally doped β-Ga_2O_3 film grown on c-sapphire substrate was measured at ≈3×10^{16} cm^{-3}. Our results show that improved electrical properties of the thin films were obtained by using the off-axis substrates. The best electrical properties were exhibited by the thin films grown on 6° off-axis sapphire using an oxygen volume percentage of 4.8%. The measured room temperature Hall mobility was 106.6 cm^{-2} V^{-1} s^{-1} with an n-type carrier concentration of 4.83×10^{17} cm^{-3}. Under the same growth condition, the measured room temperature Hall mobility for the thin films on 3.5° and 0° off-axis sapphire were 64.45 and 12.26 cm^{-2} V^{-1} s^{-1}, respectively. The Hall mobility of the thin film grown on 6° off-axis substrate was ≈9 times higher compared to the one grown on 0° off-angled substrate. The higher mobility was observed due to the reduction of the defect densities for the thin films grown on off-axis sapphire substrates. To the best of our knowledge, the electrical properties of the LPCVD grown heteroepitaxial β-Ga

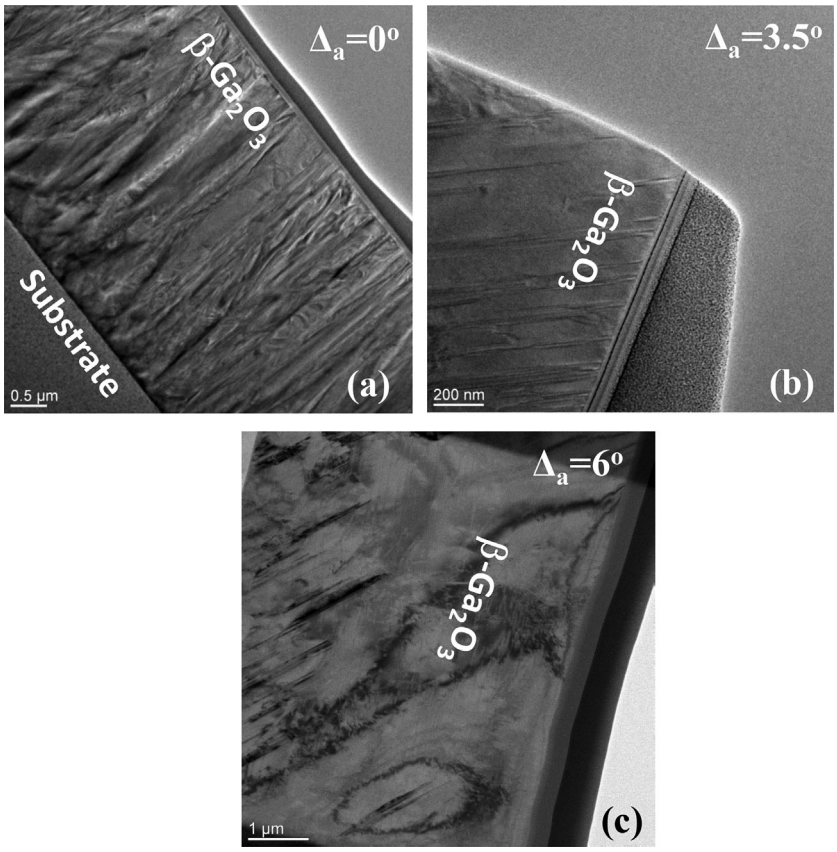

Figure 7. Cross sectional TEM images of β-Ga_2O_3 thin films grown on c-plane (0001) sapphire substrates with different off-angles toward <11–20>. a) $\Delta_a = 0°$. b) $\Delta_a = 3.5°$. c) $\Delta_a = 6°$. The thin films have a thickness of ≈6 μm.

$_2O_3$ thin films on the off-axis sapphire substrates represent the best electrical quality among the reported ones.

The temperature dependence of the n-type carrier concentration and mobility for the Si doped β-Ga_2O_3 thin films are shown in **Figure 9**a and b, respectively. Ti/Au was used as the ohmic electrode for the temperature dependent Hall measurement.[33,35] The electrodes maintained ohmic property throughout the entire temperature range. The room temperature carrier concentrations of the thin films grown on 6°, 3.5°, and 0° off-axis c-sapphire at the same growth condition with doping source flow rate of 0.01 sccm were 5×10^{17}, 3×10^{17}, and 1.5×10^{17} cm^{-3}, respectively. The thin film on 6° off-axis c-sapphire has the highest carrier concentration which can be due to the presence of lowest compensating acceptor centers or efficient incorporation of Si in the thin films grown on off-axis substrates. However further studies are needed to support our hypothesis and is beyond the scope of this paper. The estimated activation energy for Si ranges between 13.6 meV and 23 meV, which are similar to the reported values.[36,37] For the thin film grown on 6° off-axis substrate, the peak mobility of ≈238 $cm^{-2}V^{-1}s^{-1}$ occurred at 87 K, which decreased to ≈85 $cm^{-2}V^{-1}s^{-1}$ at room temperature. The peak mobility for the thin films grown on 3.5° and 0° off-axis substrates occurring at 94 and 95 K were ≈155 and ≈21 $cm^{-2}V^{-1}s^{-1}$, respectively. The nonobvious temperature dependence of carrier concentration at low temperatures ($T < 28$ K) for the three thin films could be due to the conduction in an impurity band formed by donors in the bandgap. The donor band is formed by the wave functions overlap of neighboring electrons in relatively high doped semiconductors.[38] The electrons move slowly within this band by tunneling

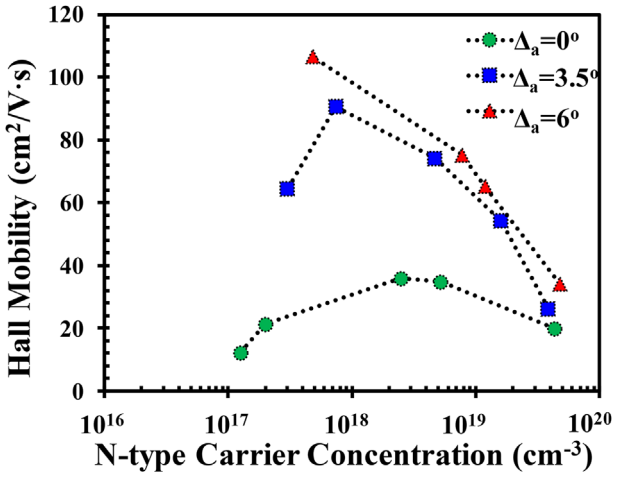

Figure 8. Electron Hall mobility as a function of carrier concentration for Si doped β-Ga_2O_3 thin films grown on c-plane (0001) sapphire substrates with different off-angles toward <11–20>. The thin films have a thickness of ≈6 μm.

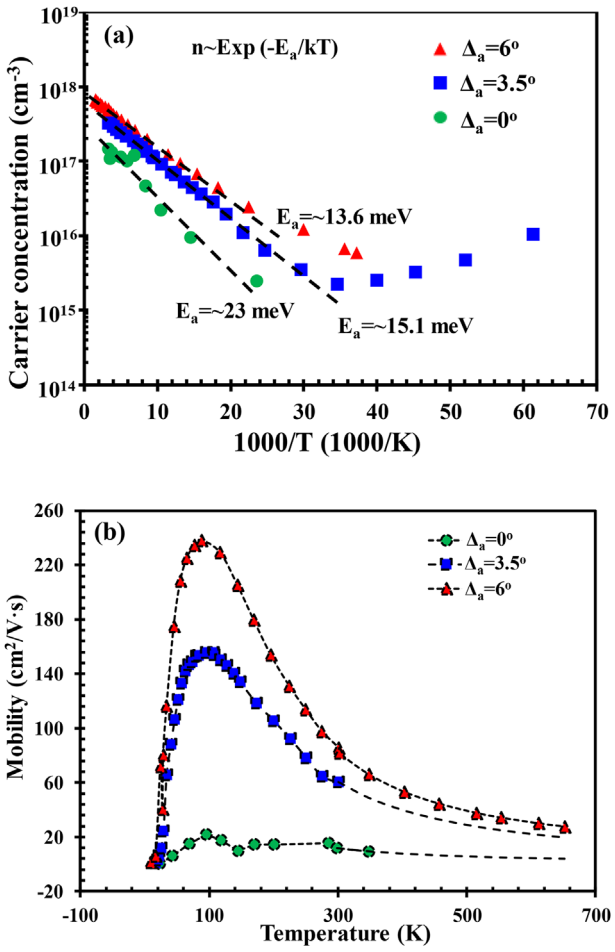

Figure 9. Temperature dependent Hall measurements for the Si doped β-Ga_2O_3 thin films grown on c-plane (0001) sapphire substrates with different off-angles toward <11–20>. a) Carrier concentration. b) Mobility. The thin films have a thickness of ≈6 μm.

or hopping. The conduction mechanism is dominated by donor band conduction at low temperatures resulting in weak increase in carrier concentration. Optical phonon scattering at high temperatures and ionized impurity scattering at low temperatures also limit the electron mobility in these thin films.[39] The thin films with the higher carrier concentrations exhibited a similar trend for the temperature dependence of the carrier, mobility and resistivity. Temperature dependence of carrier concentration and electron mobility were reported previously for Ge doped homoepitaxial (010) β-Ga_2O_3 thin film grown by MBE,[40] as well as for unintentionally doped β-Ga_2O_3 single crystal grown by EFG.[2] Temperature dependence of carrier mobility for heteroepitaxial β-Ga_2O_3 film was not reported previously.

4. Conclusion

In summary, we demonstrated fast growth rate and orientation controlled growth of heteroepitaxial β-Ga_2O_3 thin films on off-axis c-sapphire substrates by LPCVD. Effective n-type doping and doping control using Si as the dopant was achieved. The crystal orientation and phase purity of the thin films grown on sapphire substrates with different off-axis angles were established by X-ray phi scan and Raman spectroscopy measurements. Our results indicate that improved crystalline material quality and electrical properties of β-Ga_2O_3 can be achieved by using off-axis sapphire substrates. The improvement can be attributed to the strong in-plane orientation enhancement. Room temperature electron Hall mobility of 106.6 $cm^{-2}V^{-1}s^{-1}$ was obtained for a Si-doped heteroepitaxial thin film with a doping concentration of 4.83×10^{17} cm^{-3} grown on 6° off-axis c-sapphire substrate. Cost-effective production of such high quality β-Ga_2O_3 thin films by LPCVD technique will pave the way for future device applications.

Acknowledgements

Rafique, Han, and Zhao thank the funding support from the National Science Foundation (NSF) (DMR-1755479). Mou and Neal thank the funding support from the GHz-THz Electronics portfolio of the Air Force Office of Scientific Research (AFOSR). The authors would like to thank Yuewei Zhang from Prof. Siddharth Rajan's group at OSU for his assistance on the asymmetric XRD measurements for β-Ga_2O_3 samples.

Conflict of Interest

The authors declare no conflict of interest.

Keywords

gallium oxide, low pressure chemical vapor deposition, off-axis substrate

Received: July 5, 2017
Revised: August 19, 2017
Published online: November 22, 2017

[1] M. Orita, H. Ohta, M. Hirano, *Appl. Phys. Lett.* **2000**, *77*, 4166.
[2] T. Oishi, Y. Koga, K. Harada, M. Kasu, *Appl. Phys. Express* **2015**, *8*, 031101.
[3] T. C. Lovejoy, E. N. Yitamben, N. Shamir, J. Morales, E. G. Villora, K. Shimamura, S. Zheng, F. S. Ohuchi, M. A. Olmstead, *Appl. Phys. Lett.* **2009**, *94*, 081906.
[4] Z. Galazka, K. Irmscher, R. Uecker, R. Bertram, M. Pietsch, A. Kwasniewski, M. Naumann, T. Schulz, R. Schewski, D. Klimm, M. Bickermann, *J. Cryst. Growth* **2014**, *404*, 184.
[5] T. Onuma, S. Saito, K. Sasaki, T. Masui, T. Yamaguchi, T. Honda, A. Kuramata, M. Higashiwaki, *Jpn. J. Appl. Phys.* **2016**, *55*, 1202B2.
[6] R. Schewski, M. Baldini, K. Irmscher, A. Fiedler, T. Markurt, B. Neuschulz, T. Remmele, T. Schulz, G. Wagner, Z. Galazka, M. Albrecht, *J. Appl. Phys.* **2016**, *120*, 2253038.
[7] V. I. Nikolaev, A. I. Pechnikov, S. I. Stepanov, I. P. Nikitina, A. N. Smirnov, A. V. Chikiryaka, S. S. Sharofidinov, V. E. Bougrov, A. E. Romanov, *Mater. Sci. Semicond. Process.* **2016**, *47*, 16.
[8] S. Rafique, L. Han, H. Zhao, *Phys. Status Solidi A.* **2016**, *213*, 1002.
[9] H. Okumura, M. Kita, K. Sasaki, A. Kuramata, M. Higashiwaki, J. S. Speck, *Appl. Phys. Express* **2014**, *7*, 095501.
[10] G. Wagner, M. Baldini, D. Gogova, M. Schmidbauer, R. Schewski, M. Albrecht, Z. Galazka, D. Klimm, R. Fornari, *Phys. Status Solidi A* **2014**, *211*, 27.

[11] H. Murakami, K. Nomura, K. Goto, K. Sasaki, K. Kawara, Q. T. Thieu, R. Togashi, Y. Kumagai, M. Higashiwaki, A. Kuramata, S. Yamakoshi, B. Monemar, A. Koukitu, *Appl. Phys. Express* **2015**, *8*, 015503.
[12] S. Rafique, L. Han, M. J. Tadjer, J. A. Freitas Jr., N. A. Mahadik, H. Zhao, *Appl. Phys. Lett.* **2016**, *108*, 182105.
[13] D. Guo, Z. Wu, P. Li, Y. An, H. Liu, X. Guo, H. Yan, G. Wang, C. Sun, L. Li, W. Tang, *Opt. Mater. Express* **2014**, *4*, 1067.
[14] N. M. Sbrockey, T. Salagaj, E. Coleman, G. S. Tompa, Y. Moon, M. S. Kim, *J. Electron. Mater.* **2015**, *44*, 1357.
[15] W. Seiler, M. Selmane, K. Abdelouhadi, J. Perriere, *Thin Solid Films* **2015**, *589*, 556.
[16] S. Rafique, L. Han, A. T. Neal, S. Mou, M. J. Tadjer, R. H. French, H. Zhao, *Appl. Phys. Lett.* **2016**, *109*, 132103.
[17] H. W. Kim, N. H. Kim, *Mater. Sci. Eng. B* **2004**, *110*, 34.
[18] W. Mi, J. Ma, Z. Zhu, C. Luan, Y. Lv, H. Xiao, *J. Cryst. Growth* **2012**, *354*, 93.
[19] E. G. Villora, K. Shimamura, K. Kitamura, K. Aoki, *Appl. Phys. Lett.* **2006**, *88*, 031105.
[20] K. Kaneko, H. Ito, S.-D. Lee, S. Fujita, *Phys. Status Solidi C* **2013**, *10*, 1596.
[21] Y. Oshima, E. G. Villora, K. Shimamura, *J. Cryst. Growth* **2015**, *410*, 53.
[22] Z. Lin, J. Zhang, S. Xu, Z. Chen, S. Yang, K. Tian, X. Su, X. Shi, Y. Hao, *Appl. Phys. Lett.* **2014**, *105*, 082114.
[23] S. Nakagomi, Y. Kokubun, *J. Cryst. Growth* **2012**, *349*, 12.
[24] C.-T. Zhong, G.-Y. Zhang, *Rare Mater.* **2014**, *33*, 709.
[25] X. Q. Shen, H. Matsuhata, H. Okumura, *Appl. Phys. Lett.* **2005**, *86*, 021912.
[26] X. Z. Liu, P. Guo, T. Sheng, L. X. Qian, W. L. Zhang, Y. R. Li, *Opt. Mater.* **2016**, *51*, 203.
[27] Y. Chen, H. Liang, X. Xia, P. Tao, R. Shen, Y. Liu, Y. Feng, Y. Zheng, X. Li, G. Du, *J. Mater. Sci. Mater. Electron.* **2015**, *26*, 3231.
[28] M. J. Tadjer, M. A. Mastro, N. A. Mahadik, M. Currie, V. D. Wheeler, J. A. FreitaJ, Jr., J. D. Greenlee, J. K. Hite, K. D. Hobart, C. R. Eddy, Jr., F. J. Kub, *J. Electron. Mater.* **2016**, *45*.
[29] J. H. Kim, K. H. Yoon, *J. Mater. Sci. Mater. Electron.* **2009**, *20*, 879.
[30] X.-Q. Shen, M. Shimizu, H. Okumura, *Jpn. J. Appl. Phys.* **2003**, *42*, L1293.
[31] T. Jiang, S. Xu, J. Zhang, P. Li, J. Huang, Z. Ren, J. Zhu, Z. Chen, Y. Zhao, Y. Hao, *AIP Adv.* **2016**, *6*, 035316.
[32] R. Rao, A. M. Rao, B. Xu, J. Dong, S. Sharma, M. K. Sunkara, *J. Appl. Phys.* **2005**, *98*, 094312.
[33] E. Chicoidze, H. J. Von Bardeleben, K. Akaiwa, E. Shigematsu, K. Kaneko, S. Fujita, Y. Dumont, *J. Appl. Phys.* **2016**, *120*, 025109.
[34] W. S. Hwang, A. Verma, H. Peelaers, V. Protasenko, S. Rouvimov, H. Xing, A. Seabaugh, W. Haensch, C. Van De Walle, Z. Galazka, M. Albrecht, R. Fornari, D. Jena, *Appl. Phys. Lett.* **2014**, *104*, 203111.
[35] E. Ahmadi, O. S. Koksaldi, S. W. Kaun, Y. Oshima, D. B. Short, U. K. Mishra, J. S. Speck, *Appl. Phys. Express* **2017**, *10*, 041102.
[36] A. Kuramata, K. Koshi, S. Watanabe, Y. Yamaoka, T. Masui, S. Yamakoshi, *Jpn. J. Appl. Phys.* **2016**, *55*, A2.
[37] M. R. Lorenz, J. F. Woods, R. J. Gambino, *J. Phys. Chem. Solids* **1967**, *28*, 403.
[38] T. Oishi, K. Harada, Y. Koga, M. Kasu, *Jpn. J. Appl. Phys.* **2016**, *55*, 030305.
[39] M. J. Tadjer, N. A. Mahadik, V. D. Wheeler, E. R. Glaser, L. Ruppalt, A. D. Koehler, K. D. Hobart, C. R. Eddy, , Jr., F. J. Kub, *ECS J. Solid State Sci. Technol.* **2016**, *5*, P468.
[40] N. Moser, J. Mccandless, A. Crespo, K. Leedy, A. Green, A. Neal, S. Mou, E. Ahmadi, J. Speck, K. Chabak, N. Peixoto, G. Jessen, *IEEE Electron Device Lett.* **2017**, *38*, 775.

